February 2008

SOFC Anodes Based on LST–YSZ Composites and on $Y_{0.04}Ce_{0.48}ZrM_{0.48}O_2$

Guntae Kim
University of Pennsylvania

Michael D. Gross
Bucknell University

Wensheng Wang
University of Pennsylvania

John M. Vohs
University of Pennsylvania, vohs@seas.upenn.edu

Raymond J. Gorte
University of Pennsylvania, gorte@seas.upenn.edu

Follow this and additional works at: http://repository.upenn.edu/cbe_papers

SOFC Anodes Based on LST–YSZ Composites and on $Y_{0.04}Ce_{0.48}ZrM_{0.48}O_2$

Abstract

The properties of solid oxide fuel cell (SOFC) anode functional layers prepared by impregnation of 1 wt % Pd and 10 wt % ceria into porous scaffolds of either $Y_{0.04}Ce_{0.48}Zr_{0.48}O_2$ (CZY) or composites of $La_{0.3}Sr_{0.7}TiO_3$ (LST) and yttria-stabilized zirconia (YSZ) were examined to determine whether these scaffold materials would have sufficient electronic and ionic conductivity. Laminated tapes were cofired to produce 50 m YSZ electrolytes and 50 μm scaffolds, supported on LSF–YSZ cathodes. The electronic conductivities of LST–YSZ composites were a function of the porosity and the weight fraction of LST but could be sufficient for use in thin functional layers. However, anodes made with LST–YSZ composites had higher nonohmic losses than cells made with YSZ scaffolds. With CZY scaffolds, some migration of Ce into the YSZ electrolyte was observed after cofiring. While CZY exhibited electronic conductivity, the loss in ionic conductivity compared to YSZ again resulted in higher nonohmic losses. The implications of these results for producing better ceramic anodes are discussed.

Comments

SOFC Anodes Based on LST–YSZ Composites and on $Y_{0.04}Ce_{0.48}Zr_{0.48}O_2$

Guntae Kim,[a] Michael D. Gross,[b] Wensheng Wang,[a],* John M. Vohs,[a],* and Raymond J. Gorte[a],*,z

[a]*Department of Chemical and Biomolecular Engineering, University of Pennsylvania, Philadelphia, Pennsylvania 19104, USA*
[b]*Department of Chemical Engineering, Bucknell University, Lewisburg, Pennsylvania 17837, USA*

The properties of solid oxide fuel cell (SOFC) anode functional layers prepared by impregnation of 1 wt % Pd and 10 wt % ceria into porous scaffolds of either $Y_{0.04}Ce_{0.48}Zr_{0.48}O_2$ (CZY) or composites of $La_{0.3}Sr_{0.7}TiO_3$ (LST) and yttria-stabilized zirconia (YSZ) were examined to determine whether these scaffold materials would have sufficient electronic and ionic conductivity. Laminated tapes were cofired to produce 50 μm YSZ electrolytes and 50 μm scaffolds, supported on LSF–YSZ cathodes. The electronic conductivities of LST–YSZ composites were a function of the porosity and the weight fraction of LST but could be sufficient for use in thin functional layers. However, anodes made with LST–YSZ composites had higher nonohmic losses than cells made with YSZ scaffolds. With CZY scaffolds, some migration of Ce into the YSZ electrolyte was observed after cofiring. While CZY exhibited electronic conductivity, the loss in ionic conductivity compared to YSZ again resulted in higher nonohmic losses. The implications of these results for producing better ceramic anodes are discussed.
© 2008 The Electrochemical Society. [DOI: 10.1149/1.2840473] All rights reserved.

The development of high-performance ceramic anodes would provide significant advantages for solid oxide fuel cells (SOFCs). For example, unlike the more commonly used Ni-based electrodes, ceramic anodes would not promote the formation of carbon fibers when exposed to hydrocarbon fuels.[1-3] Furthermore, it is expected that ceramic electrodes would tolerate repeated oxidation and reduction cycles without fracturing. Because of these potential advantages, there have been a significant number of reports of SOFCs that use electronically conductive oxides as the main component of the anode.[4-12] In general, the performance of ceramic anodes has been modest due to their low conductivities and catalytic activities compared to Ni. Therefore, much of the effort in this area has been directed toward identifying new materials, such as in the work that led to the recent discoveries of $Sr_2Mg_{1-x}Mn_xMoO_{6-\delta}$[11] and $La_{0.75}Sr_{0.25}Cr_{0.5}Mn_{0.5}O_3$.[12]

In our laboratory, the focus has been on developing ceramic anodes that have separate functional and conduction layers so that different materials may be used for conductivity and electrocatalysis.[13-15] Because the electrochemical reactions occur only in the functional layer, the conduction layer can be essentially any porous material which has a high electronic conductivity. This concept has been demonstrated in a previous study in which the electrode performance was found to be essentially the same when the conduction layer was made from either Ag paste or a porous layer of $La_{0.7}Sr_{0.3}TiO_3$ (LST).[13] For the functional layer, we have focused on materials that are good oxidation catalysts (e.g., transition-metal-doped ceria). The conductivity of the functional layer can be modest if this layer is thin. In our past work, electronic conductivity was achieved by impregnating relatively high loadings of ceria (40–60 wt %) into a porous layer of yttria-stabilized zirconia (YSZ). Even though the conductivity of the functional layer in the fresh cell was <0.02 S/cm in humidified H_2 at 973 K, ohmic losses in the anode were acceptable in the freshly prepared cells because the functional layers were only 12 μm thick. The total anode losses, including the ohmic contribution, for a cell with a functional layer made by impregnating 1 wt % Pd and 40 wt % ceria into a 12 μm thick, porous YSZ, were 0.26 Ω cm² in humidified H_2 at 973 K.[13] Unfortunately, long-time aging or heating to 1173 K caused the conductivity of the functional layer to decrease, apparently due to changes in the ceria film.[14]

The goal of the present work was to modify the functional layer by replacing the porous YSZ with materials that have electronic conductivity, with the goal of further enhancing the performance of the multilayered anode. Metal-doped ceria was still added to the porous layer by impregnation but only to provide catalytic activity. Two strategies were investigated for achieving conductivity. First, the porous YSZ was replaced with a porous mixture of LST and YSZ. LST–YSZ mixtures remain as separate phases, even after calcination at 1773 K,[16] so that porous composites can have both electronic conductivity (from the LST) and ionic conductivity (from the YSZ). This approach is similar to that used in two earlier studies, which employed porous mixtures of YSZ and $Sr_{0.92}Y_{0.08}TiO_3$ (YST) as the backbone for the anode.[17,18] LST was chosen for the present study because it has slightly higher conductivity than YST[19] and is similarly unreactive with YSZ. The effects on conductivity of the LST–YSZ composition and of the composite porosity were also examined. In the second approach, the porous YSZ was replaced with porous $Y_{0.04}Ce_{0.48}Zr_{0.48}O_2$ (CZY). CZY was found to remain as a single-phase material after high-temperature calcination and exhibited electronic conductivity under reducing conditions due to the reduction of Ce^{+4}. Because solid solutions of ceria and zirconia reduce more easily than pure ceria[20-22] or ceria doped with other rare earths, such as Sm^{+3} or Y^{+3},[23] it was expected that CZY would have good conductivity under reducing conditions.

It will be shown that both approaches, preparing porous functional layers by impregnating catalysts into LST–YSZ composites or into CZY, can help stabilize the ohmic losses in cells. However, replacing YSZ with either an LST–YSZ composite or CZY results in a loss of ionic conductivity that decreases the overall performance of the electrode.

Experimental

The YSZ used in this study was obtained from Tosoh (8 mol % Y_2O_3-doped ZrO_2). The LST and CZY powders were prepared in our laboratory using procedures that have been described in detail elsewhere.[13,20] The LST was prepared by solid-state reaction of $La(NO_3)_3·6H_2O$, $Sr(NO_3)_2$ and TiO_2 at 1273 K, while the CZY was prepared using the Pechini method to ensure formation of a single-phase material, with an initial calcination temperature of 723 K.

Cell fabrication was similar to that used in previous studies,[13,24] except that the porous YSZ in the anode was replaced with either a porous mixture of LST and YSZ or with porous CZY. The cells were made by first fabricating a three-layer ceramic wafer, with two porous layers separated by a dense YSZ electrolyte layer. The electrolytes in the cells based on LST–YSZ were 75 μm thick, while the

electrolytes were 50 μm thick in the cells based on CZY. The three-layer ceramic wafers were produced by laminating three green ceramic tapes, synthesized by tape casting, with pore formers in the two outer tapes. The laminated, green tapes were fired to 1773 K to produce the final ceramic structures. The porous layer on one side of the electrolyte was 300 μm thick YSZ ($\sim$65% porous) and was used as the scaffold for the LSF–YSZ ($La_{0.8}Sr_{0.2}FeO_3$) cathodes.[25] The cathodes were synthesized by impregnating the porous YSZ with an aqueous solution containing $La(NO_3)_3 \cdot 6H_2O$, $Sr(NO_3)_2$, and $Fe(NO_3)_3 \cdot 9H_2O$, to a loading of 40 wt % LSF, followed by calcination to 1123 K.[25,26] Previous studies have shown that the impedance of LSF–YSZ cathodes prepared in this way is between 0.1 and 0.15 Ω cm^2 at 973 K and is independent of current density.[26]

The other porous layer was used as the scaffold for the anode. Although the thicknesses, compositions, and porosities of this layer were varied, we added 10 wt % ceria and 1 wt % Pd, unless otherwise stated, so as to provide catalytic activity to the anode. Because 10 wt % ceria is insufficient to provide significant electronic conductivity,[14] essentially all of the electronic conductivity in these layers came from the scaffold structure (i.e., the porous LST–YSZ composite or porous CZY). The porosity of the functional layers was controlled by the amount of graphite pore former that was added to the initial slurry and was measured by the weight of water uptake in the sample when submersed.[27] Finally, Ag paste and Ag wire were applied to both the anode and cathode sides for current collection.

The conductivities of the porous LST–YSZ composites were measured as a function of temperature in humidified (3% H_2O) H_2 using standard, four-probe measurements on slabs that were 1$\times$1$\times$10 mm in size. The slabs were prepared from the same slurries used in tape casting the porous anode layers. Although the electronic conductivity of LST is known to increase dramatically after high-temperature reduction in very dry H_2,[28] it seems unlikely that this high conductivity would be maintained under practical operating conditions. Therefore, conductivities were measured at the lower temperatures first, prior to having the sample exposed to reducing conditions at higher temperatures.

For fuel cell testing, cells were attached to an alumina tube with a ceramic adhesive (Aremco, Ceramabond 552). The fuel to the anode was humidified (3% H_2O) H_2, and the cathode was simply exposed to air. Impedance spectra were measured at open circuit in the galvanostatic mode with a frequency range of 0.1 Hz to 100 kHz and a 5 mV ac perturbation using a Gamry Instruments potentiostat. The active area of the cells, equal to the anode area, was 0.35 cm^2, but the area of the electrolyte and cathode was $\sim$1 cm^2. Because the conductivity of YSZ electrolytes is well documented and because losses associated with LSF–YSZ cathodes made by impregnation are low (between 0.1 and 0.15 Ω cm^2 at 973 K[26]), anode losses could be estimated without solving the difficulties associated with reference electrodes.[29]

Results

LST–YSZ composites.— Figure 1 shows a scanning electron microscope (SEM) image of the interface between a dense YSZ electrolyte and a 50:50 LST–YSZ composite having 55% porosity [LST–YSZ(50:50,55)]. The LST–YSZ composite has a similar appearance to structures obtained with pure YSZ using the same pore formers and tape-casting procedures,[27] suggesting that the porosity and pore structure are again established by the amount and type of pore formers. In agreement with this, the porosity of LST–YSZ composites could be controlled by varying the amounts of graphite pore formers that were added. For example, ceramic tapes made using LST and YSZ powders, but without the addition of pore formers, produced dense composites.[16] However, because of the low reactivity of LST with YSZ,[16] the porous LST–YSZ composite is not as well connected to the dense YSZ electrolyte as porous YSZ was with dense YSZ.
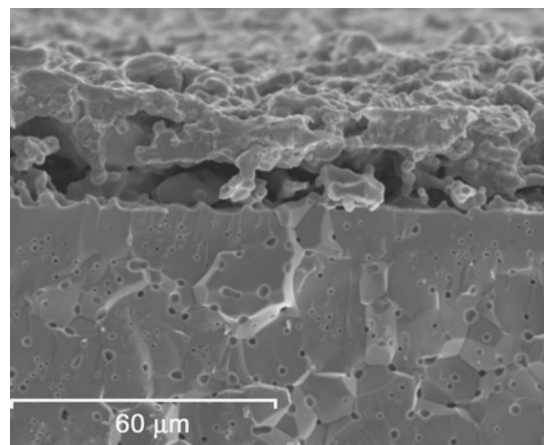

Figure 1. SEM image of LST–YSZ(50:50;55) composite near the interface with the YSZ electrolyte.

The LST–YSZ(50:50,55) composite was found to have a conductivity of 0.006 S/cm at 973 K in humidified H_2. Because the conductivity of a YSZ slab having a similar porosity and structure was only 0.001 S/cm,[30] the conductivity of the LST–YSZ composite comes primarily from the LST and must therefore be electronic, rather than ionic. Note the conductivity of dense YSZ at 973 K is 0.021 S/cm and almost purely ionic.[31] However, a conductivity of 0.006 S/cm is not sufficient for this application. For the ohmic losses in a functional layer made from a material with a conductivity of 0.006 S/cm to be 0.1 Ω cm^2 (note that we arbitrarily choose 0.1 Ω cm^2 as an acceptable loss), the thickness would need to be 6 μm. In general, the conductivity of a composite will depend on its porosity and the mass fraction of the conducting phase. In the LST–YSZ(50:50,55) composite, the volume fraction of LST is only 22.5 vol %, which is well below the percolation threshold of 30 vol % required for conductivity in random media.

To achieve higher conductivities, we prepared composites with the same composition but lower porosity [50:50 LST–YSZ, 30% porosity, [LST–YSZ(50:50,30)] and composites with higher mass fraction of LST (75:25 LST–YSZ, 50% porosity, [LST–YSZ(75:25,50)]. The conductivities of these materials, along with that of the initial slab, are shown as a function of temperature in Fig. 2. The measurements were initially performed at lower temperatures, after holding the sample in humidified H_2 for 30 min, to avoid measuring the potentially unstable conductivities reported following high-temperature reduction of LST. The conductivities of the LST–YSZ(50:50,30) and LST–YSZ(75:25,50) composites were significantly higher than that of LST–YSZ(50:50,55), with values near 0.03 S/cm at 973 K. The similarity in the conductivities of these two composites is likely because the volume percents of LST, 35 and 37.5%, are also similar. Pretreating the LST-YSZ(75:25,50) composite by heating it to 1173 K in humidified H_2 further increased its conductivity at 973 K to $\sim$ 0.07 S/cm. Although the conductivities of the composites remained too low for using them as the conduction layer of the electrode, a conductivity of 0.03 S/cm should be sufficient for use in functional layers thinner than 30 μm.

Electrodes based on LST–YSZ(50:50,55).— Fuel cells were prepared from each of the three LST–YSZ composites, using identical LSF–YSZ cathodes and 75 μm YSZ electrolytes. Table I lists the maximum power density, conductivity, and ohmic and nonohmic parts of the area-specific resistance (ASR) for all of the cells used in this study. Even though previous work has shown that good performance can be obtained with a 12 μm functional layer,[13] the anode functional layers in the present study were chosen to be 35 μm thick because the focus was on measuring the ohmic contributions of the anodes. Then, 10 wt % ceria and 1 wt % Pd were added to the an-
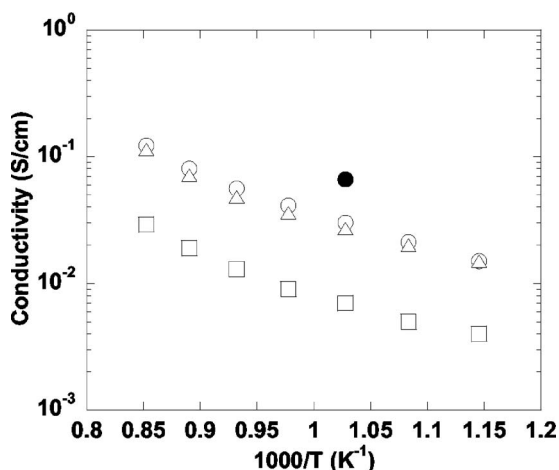
Figure 2. Conductivity of LST–YSZ composites as a function of temperature: (○) LST-YSZ(75,25;50); (△) LST–YSZ(50:50; 30); (□) LST-YSZ(50:50;55). The data were obtained in humidified (3% H_2O) H_2, starting at the lower temperatures. ● was obtained after heating in humidified H_2 to 1173 K.

Figure 3. *V-I* polarization curves in humidified H_2 for a cell made by impregnating 1 wt % Pd and 10 wt % ceria into a 50 μm layer of the LST–YSZ(50:50;55) composite at the following temperatures: (○) at 973 K, (△) at 1073 K, and (◇) at 1173 K.

odes for catalytic purposes and Ag paste was used for current collection. Figure 3 shows the *V-I* polarization curves for a cell made with the LST–YSZ(50:50;55) composite, operating on humidified (3% H_2O) H_2 at 973, 1073, and 1173 K. The OCV were close to the Nernst potentials in each case and the maximum power densities were 0.20, 0.43, and 0.64 W/cm^{2} at 973, 1073, and 1173 K, respectively.

Impedance data at the open-circuit voltage (OCV), at 973 K, are shown in Fig. 4. The data are shown for the cell after it was initially heated to 973 K and again at 973 K after briefly heating to 1073 and 1173 K. Immediately after reaching 973 K, the ohmic loss in the cell was 1.1 Ω cm[2] and this increased only slightly after heat-treatment. Based on the calculated resistance of the 75 μm electrolyte at 973 K, 0.36 Ω cm[2], the ohmic contribution of 35 μm, LST–YSZ(50:50;55) composite to the impedance in Fig. 3 was 0.74 Ω cm[2]. This implies that the conductivity of the LST–YSZ(50:50;55) composite is 0.0047 S/cm, a value similar to that determined from the conductivity measurements in Fig. 2.

A major problem encountered in a previous study using impregnated ceria for conductivity in a YSZ-based functional layer was that the conductivity of the ceria decreased on heating to higher temperatures.[14] The ohmic losses at 973 K of a cell with a 12 μm thick functional layer containing 20 wt % ceria and 1 wt % Pd increased by 0.11 Ω cm[2], which indicates the conductivity decreased by almost a factor of two, after only 2 h of operation at 1073 K. The fact that heating to 1173 K caused minimal changes in the ohmic losses in Fig. 4 is another strong indication that the LST–YSZ composite, rather than the impregnated ceria, is providing the electronic conductivity.
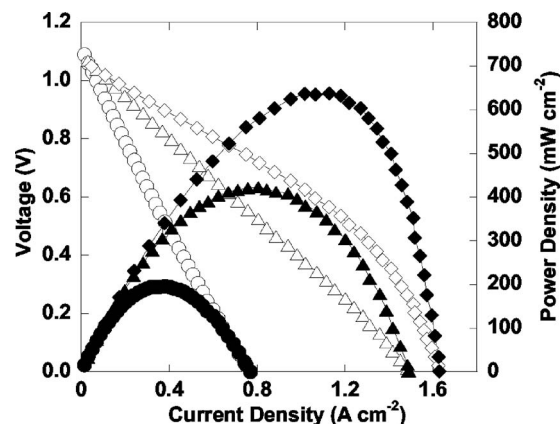
Obviously, the performance of the cell made from the LST–YSZ(50:50,55) composite was not very good, with a total-cell ASR at 973 K that was >1.6 Ω cm[2], even before heating. Although the low performance is due, in part, to the high ohmic losses, the nonohmic losses were also high and increased, from ~0.5 Ω cm[2], initially, to 0.9 Ω cm[2] after heating to 1173 K. Because the LSF–YSZ cathode losses are estimated to be only 0.1–0.15 Ω cm[2],[26] the poor performance is mostly due to the anode. It is noteworthy that the initial, total-cell, nonohmic losses at 973 K were only 0.2 Ω cm[2] for a cell in which the functional layer was prepared by impregnating ceria and Pd into 50 μm thick, porous YSZ.[14]

Electrodes based on LST–YSZ(75:25,50).— The effect of changing the weight fraction of LST within the composite was tested by studying a cell made with a 35 μm thick layer of the LST–YSZ(75:25,50) composite, again using 10 wt % ceria and 1 wt % Pd for catalytic activity. The maximum power densities for this cell were 0.25, 0.57, and 0.90 W/cm^{2} at 973, 1073, and 1173 K, respectively. These values are higher than that obtained for the cell made with the LST–YSZ(50:50,55) composite, but not dramatically so. Figure 5 shows the impedance data at 973 K for this cell, initially and after testing at 1073 and 1173 K. The nonohmic losses again increased after high-temperature treatment. More important for this discussion, the total ohmic losses were 0.8 Ω cm[2], initially, and after heat-treatment. After subtracting the electrolyte contribution (0.36 Ω cm[2]), the ohmic contribution from the anode is determined to be 0.44 Ω cm[2]. Based on the same arguments used in calculating the conductivity of the LST–YSZ(50:50,55) composite, the conductivity of the LST–YSZ(75:25,50) composite is only 0.008 S/cm, a factor of four lower than that determined from four-probe slab measurements. To check the reproducibility of the LST–YSZ(75:25,50), fuel cell conductivity, an otherwise identical fuel cell was prepared

Table I. Summary of the experimental results (in humidified H_2, at 973 K).

Anode scaffold	Conductivity[a] (S/cm)	Conductivity[b] (S/cm)	R_{ohmic} (Ω cm^{-2})	$R_{nonohmic}$ (Ω cm^{-2})	Power density (W/cm^{2})
LST–YSZ(50:50;55)	0.006	0.0047	0.74	0.5	0.20
LST–YSZ(50:50;30)	0.03	0.006	0.57	0.6	0.23
LST–YSZ(75:25;50)	0.027	0.008	0.44	0.6	0.25
CZY		0.0063	0.80	2.0	0.08

[a] Conductivities measured by four-probe method.
[b] Conductivities calculated from impedance measurements.

Figure 4. Impedance spectra for the cell made by impregnating 1 wt % Pd and 10 wt % ceria into a 50 μm layer of the LST–YSZ(50:50;55) composite at 973 K: ($\bigcirc$) initial results, ($\triangle$) after heating briefly to 1073 K and returning to 973 K, ($\diamond$) after heating briefly to 1173 K and returning to 973 K.
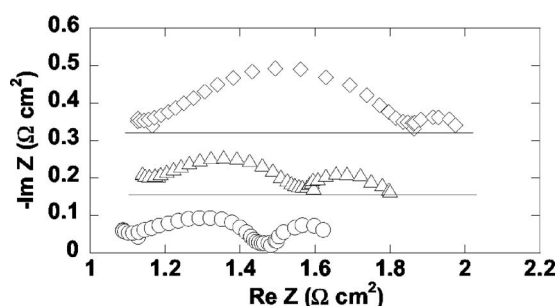

Figure 6. Impedance spectra for the cell made by impregnating 1 wt % Pd and 10 wt % ceria into a 50 μm layer of the LST–YSZ(50:50;30) composite at 973 K: ($\bigcirc$) initial results; ($\triangle$) after heating briefly to 1073 K and returning to 973 K; ($\diamond$) after heating briefly to 1173 K and returning to 973 K.

with a 20 μm thick layer of the LST–YSZ(75:25,50) composite, again using 10 wt % ceria and 1 wt % Pd. At 973 K in humidified H_2, the cell with the 20 μm functional layer exhibited an initial maximum power density of 350 mW/cm^2 and a total ohmic loss of 0.55 Ω cm^2. When the expected ohmic contribution from the electrolyte, 0.36 Ω cm^2, is subtracted from the total ohmic loss of 0.55 Ω cm^2, the conductivity of the LST–YSZ(75:25,50) composite is calculated to be 0.011 S/cm, close to the value obtained with the thicker functional layer. The discrepancy in the conductivities determined from fuel cell data and from four-probe measurements may be related to the poor interface between the YSZ electrolyte and LST–YSZ composite, as shown in Fig. 1.

Because the nonohmic losses in the cell using the LST–YSZ(75:25,50) composite were also much larger than had been obtained previously using a cell made with porous YSZ that was 50 μm thick, but with 40 wt % ceria and 1 wt % Pd,[14] the effect of ceria loading on cell performance was examined. A cell was prepared with the LST–YSZ(75:25,50) composite, 35 μm thick, but with 40 wt % ceria and 1 wt % Pd. The increased ceria loading had no impact on cell performance. The maximum power densities on the cell with 40 wt % ceria were 0.27, 0.60, and 0.93 W/cm^2 at 973, 1073, and 1173 K. This implies that cell performance with the LST–YSZ(75:25,50) composite was not limited by the amount of catalyst that was added.

Electrodes based on LST–YSZ(50:50,30).— A possible explanation for why the nonohmic losses in the cells made using LST–YSZ composites are large is that LST–YSZ(50:50,55) and LST–YSZ(75:25,50) likely have low ionic conductivity. Ionic conductivity is important for good electrode performance, and the total volume fractions of YSZ in these two composites are only 22 and 13 vol %, respectively. For a composite to have both high ionic and electronic conductivities, it should have high volume fractions for
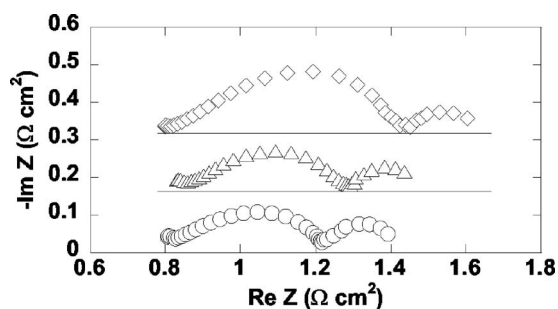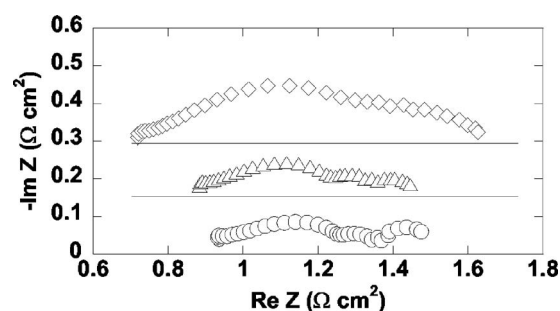
both LST and YSZ phases. Therefore, we examined a cell with the LST–YSZ(50:50,30) composite, for which the volume fractions of both phases are ~35%. As before, 10 wt % ceria and 1 wt % Pd were added to the functional layer to provide catalytic activity. Again, the *V-I* curves in humidified H_2 were essentially straight lines, with OCV close to the Nernst potential, and the maximum power densities were 0.23, 0.51, and 0.75 W/cm^2 at 973, 1073, and 1173 K, respectively.

The impedance data for this cell at 973 K in humidified H_2, initially and after heating briefly to 1073 and 1173 K, are reported in Fig. 6. The ohmic losses were initially 0.93 Ω cm^2, but this value dropped after heating to higher temperatures, to 0.88 Ω cm^2 after 1073 K and 0.72 Ω cm^2 after 1173 K. Although the conductivity of the LST–YSZ(50:50,30) composite, calculated from the initial ohmic-loss data, is again lower than the value obtained from four-probe measurements (0.006 S/cm vs 0.03 S/cm), the fact that the conductivity of the composite increases after high-temperature treatment is consistent with the usual observations for LST.[28] The initial nonohmic contribution to the cell ASR was 0.5 Ω cm^2, which is only slightly better than the results with the cells made from the LST–YSZ(75:25,50) composite. The nonohmic losses again increased dramatically after high-temperature treatments.

CZY-based functional layers.— There would be obvious advantages to a single-phase, porous layer that had both ionic and electronic conductivity. Ceria has good ionic conductivity and is somewhat electronically conductive at the $P(O_2)$ conditions observed in SOFC anodes because it is partially reduced; however, initial attempts in our laboratory to cofire a porous layer of Sm-doped ceria (SDC) together with a relatively thin, dense layer of YSZ were not successful due to the dissimilar properties of SDC and YSZ. Therefore, we chose to examine functional layers based on porous ceria-zirconia solutions. Because solid solutions with the composition $Ce_{0.5}Zr_{0.5}O_2$ undergo phase separation into ceria- and zirconia-rich phases upon calcination above 1323 K,[22] materials for this study were doped with 2 mol % Y_2O_3 ($Y_{0.04}Ce_{0.48}Zr_{0.48}O_2$). Without the addition of yttria, a ceramic wafer made from $Ce_{0.5}Zr_{0.5}O_2$ fractured into small pieces under reducing conditions, probably due to different lattice expansions in the ceria- and zirconia-rich phases. By contrast, CZY remained single phase based on x-ray diffraction, even after calcination to 1823 K. Ceramic wafers made from CZY were also found to be stable under reducing conditions.

Recent thermodynamic measurements have shown that ceria-zirconia solid solutions are reduced to a considerably greater extent than is ceria at $P(O_2)$ relevant to SOFC anodes,[20-22] suggesting that the solid solutions should show reasonable electronic conductivity under reducing conditions. In agreement with this, a dense CZY wafer was found to exhibit a conductivity of 0.2 S/cm at 973 K in humidified (3% H_2O) H_2. The conductivities of porous CZY were not measured directly, but, based on previous results with porous

Figure 5. Impedance spectra for the cell made by impregnating 1 wt % Pd and 10 wt % ceria into a 50 μm layer of the LST–YSZ(75:25;50) composite at 973 K: ($\bigcirc$) initial results, ($\triangle$) after heating briefly to 1073 K and returning to 973 K, ($\diamond$) after heating briefly to 1173 K and returning to 973 K.

Figure 8. Energy dispersive X-ray results showing the Ce content as a function of distance into the dense layer.

at 973 K and 110 mW/cm² at 1073 K, much lower than was obtained in any of the cells based on LST–YSZ composites. The impedance data in Fig. 9b shows that the ohmic losses at 973 K are 1.1 Ω cm², similar to the value observed for the cell made with the LST–YSZ(50:50;55) composite. Assuming that the ohmic losses above that expected for the electrolyte are all from the anode layer, the conductivity of porous CZY at 973 K would be 0.0063 S/cm. Although this conductivity could be increased by decreasing the porosity, it is the nonohmic losses that are a bigger concern. The nonohmic losses were more than 2 Ω cm² at 973 K and almost 1.6 Ω cm² at 1073 K.

There are two possible reasons for the large nonohmic losses. First, the diffusion of Ce ions into the electrolyte could create a dense, electronically conductive layer that effectively separates the YSZ in the electrolyte from the surface sites of the porous anode.
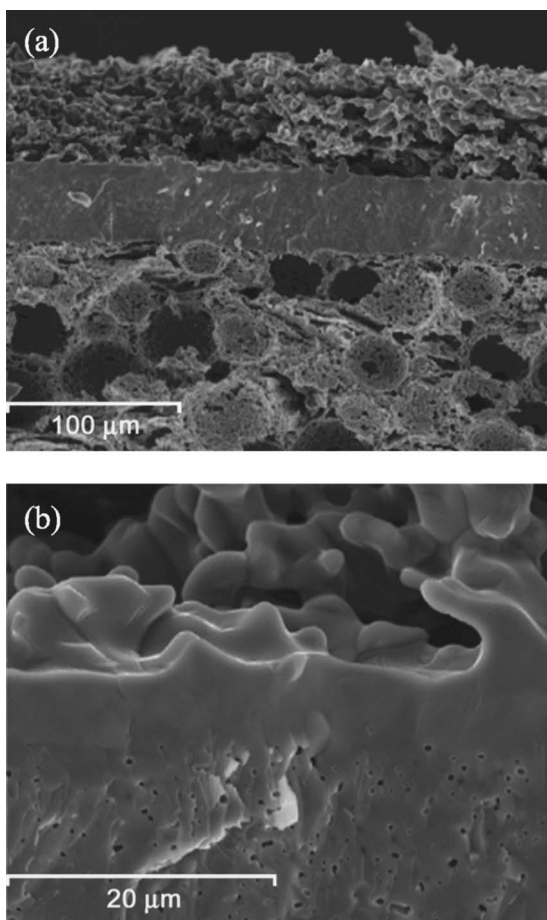
Figure 7. SEM images of a cross section of a ceramic wafer used to make a fuel cell with a CZY functional layer: (a) Image showing the CZY layer at the top and a porous YSZ layer (used to make the cathode) at the bottom, separated by a dense layer of YSZ and (b) close-up image of the CZY–YSZ interface.

YSZ,[30] structures that are 65% porous will have a conductivity that is a factor of ~20 lower, so that CZY could have sufficient conductivity for a 10 μm electrode.

Figure 7 provides SEM images of the three-layer structure used in making cells from the CZY-based anodes. The CZY layer in this image was 65% porous, as determined by water-uptake measurements. The low-magnification image in Fig. 7a shows the dense YSZ electrolyte separating the porous CZY at the top from the porous YSZ at the bottom. The pore structure of the two porous layers is different because different pore formers were used, and the image at this magnification is indistinguishable from those in which both porous layers were made from YSZ. Closer examination of the CZY–YSZ interface, Fig. 7b, shows that the dense region close to the porous CZY has fewer voids and a different texture compared to the YSZ electrolyte farther from the CZY interface. Energy dispersive X-ray analysis of the dense layer, shown in Fig. 8, indicates that Ce ions have diffused into this region, penetrating to a depth of ~10 μm. This penetration of cerium ions into the electrolyte is obviously a concern, both because of its effect on the electrolyte and because cerium is likely to be depleted from the CZY near the electrolyte interface.

The *V-I* polarization and OCV impedance curves for a cell with an anode made from 50 μm thick CZY, impregnated with 10 wt % ceria and 1 wt % Pd, are reported in Fig. 9 for operation in humidified H₂ at 973 and 1073 K. The *V-I* polarization curves in Fig. 9a are again straight, and the OCV are close to the theoretical Nernst potentials. However, the power densities are very low, 80 mW/cm²
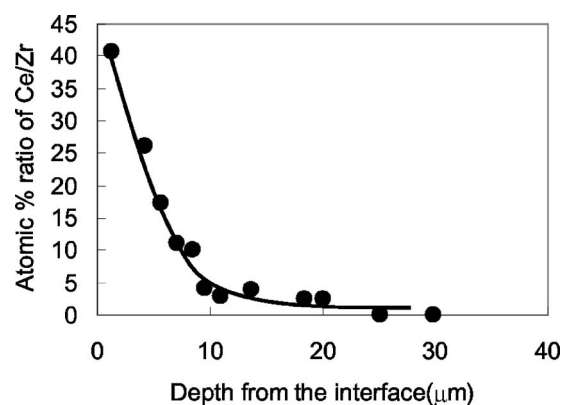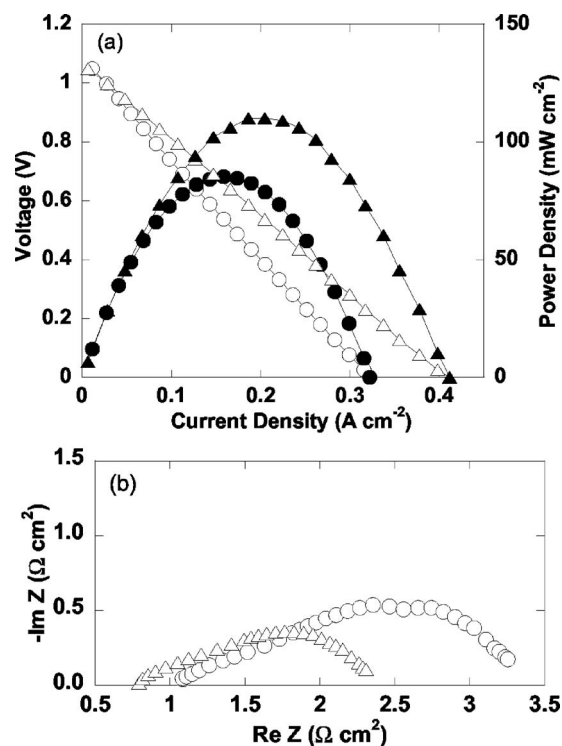

Figure 9. (a) *V-I* polarization and (b) impedance spectra for a cell made by impregnating 1 wt % Pd and 10 wt % ceria into a 50 μm layer of CZY. The data were taken in humidified H₂ (3% H₂O) at the following temperatures: (○) at 973 K and (△) at 1073 K.

The absence of an electrical potential in this electronically conductive layer would decrease the mobility of the ions and be observed as nonohmic losses. Alternatively, the porous CZY may be ineffective, either due to poor catalytic activity or poor ionic conductivity. Because ceria-zirconia solid solutions are good oxidation catalysts, poor catalytic activity is unlikely to play a role. To distinguish the two mechanisms, we prepared a cell with a 50 μm thick CZY anode layer and impregnated it with 40 wt % ceria and 1 wt % Pd. If the nonohmic losses were due to a dense layer over the electrolyte, the addition of more ceria to the anode structure should have no influence on performance, while the addition of more ceria could affect ionic conductivity and catalytic activity in the porous structure. The addition of ceria caused the total nonohmic loss at 973 K to drop to a value of ~0.5 Ω cm^2, implying that the poor performance of the CZY-based anodes is associated with the properties of the porous structure.

The reason for the poor performance of the CZY structure is likely poor ionic conductivity. The total conductivity of $Y_{0.2}Ce_{0.4}Zr_{0.4}O_{1.9}$ at 973 K in air has been reported to be 10^{-3} S/cm,[32] compared to 0.021 for YSZ. Because the electronic conductivity of CZY is likely negligible under oxidizing conditions, the ionic conductivity of CZY appears to be a factor of 20 lower than the ionic conductivity of YSZ at this temperature. As pointed out earlier, high ionic conductivity is crucial for good electrode performance.

Discussion

In high-performance electrodes, structure and composition are equally important. Although an electrode must be made from materials that have catalytic activity and are conductive, the best electrodes have ion-conducting channels extending from the electrolyte, into the electrode, to increase the concentration of three-phase-boundary sites.[33] For example, with optimized Ni–YSZ composite anodes, one important function of the YSZ is to provide the ion-conducting channels. The conventional synthesis of Ni–YSZ anodes involves cofiring mixtures of NiO and YSZ, together with the YSZ electrolyte, to produce those channels.

The structural goal for electrodes prepared by impregnation are the same, but the synthesis by impregnation allows the structure to be controlled in a more straightforward manner in that each component of the electrode is added separately, starting with the scaffold material into which the other components of the electrode are added. In past work from our laboratory, the scaffold material was generally the purely ionic conductor, YSZ.[3] Electronic conductivity and catalytic activity were added to the electrode by coating the scaffold with the components required for those functions. In the present study, we have made the scaffold of oxide materials that have both ionic and electronic conductivity. This eliminates the need to impregnate components for electronic conductivity.

For scaffolds made from either LST–YSZ or CZY, the electronic conductivity could have been sufficient for use with thin functional layers. Extrapolating to 10 μm thick electrodes, it seems feasible that the ohmic losses could be reduced to <0.1 Ω cm^2 at 973 K. However, nonohmic losses in the electrodes were always significantly larger than was observed for cells made from YSZ scaffolds. The loss in performance appears to result from the loss of ionic conductivity. In the LST–YSZ composites, the ionic conductivity is lower because the volume fraction of YSZ is lower. Although CZY has some ionic conductivity, it appears to be much lower than that of YSZ.

It is significant that the best anode performance achieved in our laboratory to date was with an electrode composed of Pd-doped ceria coating a YSZ scaffold.[13,14] In that case, ceria played the role of both catalyst and electronic conductor. With 40 wt % ceria, nonohmic losses in these cells were <0.1 Ω cm^2 in humidified H$_2$ at 973 K, even when the ohmic losses were large due to ceria providing insufficient electronic conductivity for the thickness of the anode functional layer. With 20 wt % ceria, the nonohmic losses were still only 0.2 Ω cm^2, a value much lower than was observed for any of

the electrodes prepared as part of the present study. The implication seems to be that the electrode performance is better when the scaffold is simply optimized for ionic conductivity and then coated with an electronic conductor. In the case of the LST–YSZ composites, this would suggest that improved performance could be achieved by coating a YSZ scaffold with LST and a catalyst.

Although we did not test any of the cells in this study for tolerance to redox cycling or carbon formation in dry hydrocarbons, all of the electrodes described in this paper would almost certainly have properties superior to conventional Ni-based anodes. None of the materials used in these electrodes are catalysts for carbon fiber formation in the way that Ni is. There may be some expansion and contraction of CZY under oxidizing and reducing conditions, but the effect would certainly be negligible compared to what occurs in Ni cermets.

Finally, it should be recognized that research on the preparation of electrodes by impregnation methods is still in its infancy. By impregnating electrode components into a presintered scaffold, a wide range of materials can be used that would normally undergo solid-state reactions with the electrolyte at the sintering temperature. Even with a common materials set (e.g., LST, ceria, and YSZ), one can prepare electrodes with very different structures, depending on how each component is added. This remains a promising approach for the development of high-performance electrodes.

Conclusions

Anode functional layers can be prepared by impregnating a Pd/ceria catalyst into mixing-conducting scaffolds, such as CZY or LST–YSZ composites. However, the electrodes prepared with scaffolds of porous CZY or LST–YSZ composites exhibit higher nonohmic losses than electrodes in which ceria is impregnated into porous YSZ. The critical difference is the lower ionic conductivity of the CZY and LST–YSZ scaffolds.

References

1. S. McIntosh and R. J. Gorte, *Chem. Rev. (Washington, D.C.)*, **104**, 4845 (2004).
2. T. Kim, G. Liu, M. Boaro, S.-I. Lee, J. M. Vohs, R. J. Gorte, O. H. Al-Madhi, and B. O. Dabbousi, *J. Power Sources*, **155**, 231 (2006).
3. R. J. Gorte, S. Park, J. M. Vohs, and C. Wang, *Adv. Mater. (Weinheim, Ger.)*, **19**, 1465 (2000).
4. J. Liu, B. D. Madsen, A. Ji, and S. A. Barnett, *Electrochem. Solid-State Lett.*, **5**, A122 (2002).
5. O. A. Marina, N. L. Canfield, and J. W. Stevenson, *Solid State Ionics*, **149**, 21 (2002).
6. J. Sfeir, J. van Herle, and A. J. McEvoy, *J. Eur. Ceram. Soc.*, **19**, 897 (1999).
7. Y. H. Huang, R. I. Dass, J. C. Denyszyn, and J. B. Goodenough, *J. Electrochem. Soc.*, **153**, A1266 (2006).
8. R. Mukundan, E. L. Brosha, and F. H. Garzon, *Electrochem. Solid-State Lett.*, **7**, A5 (2004).
9. J. W. Fergus, *Solid State Ionics*, **177**, 1529 (2006).
10. Q. X. Fu, F. Tietz, and D. Stover, *J. Electrochem. Soc.*, **153**, D74 (2006).
11. Y.-H. Huang, R. I. Dass, Z.-L. Xing, and J. B. Goodenough, *Science*, **312**, 254 (2006).
12. S. Tao and J. T. S. Irvine, *Nat. Mater.*, **2**, 320 (2003).
13. M. D. Gross, J. M. Vohs, and R. J. Gorte, *Electrochem. Solid-State Lett.*, **10**, B65 (2007).
14. M. D. Gross, J. M. Vohs, and R. J. Gorte, *J. Electrochem. Soc.*, **154**, B694 (2007).
15. M. D. Gross, J. M. Vohs, and R. J. Gorte, *J. Mater. Chem.*, **17**, 3071 (2007).
16. K. Ahn, S. Jung, J. M. Vohs, and R. J. Gorte, *Ceram. Int.*, **33**, 1065 (2007).
17. H. He, Y. Huang, J. M. Vohs, and R. J. Gorte, *Solid State Ionics*, **175**, 171 (2004).
18. H. Kurokawa, L. Yang, C. P. Jacobson, L. C. De Jonghe, and S. J. Visco, *J. Power Sources*, **164**, 510 (2007).
19. T. Kolodiazhnyi and A. Petric, *J. Electroceram.*, **15**, 5 (2005).
20. T. Kim, J. M. Vohs, and R. J. Gorte, *Ind. Eng. Chem. Res.*, **45**, 5561 (2006).
21. P. R. Shah, T. Kim, G. Zhou, P. Fornasiero, and R. J. Gorte, *Chem. Mater.*, **18**,

5363 (2006).
22. G. Zhou, P. R. Shah, T. Kim, P. Fornasiero, and R. J. Gorte, *Catal. Today*, **123**, 86 (2007).
23. G. Zhou, P. R. Shah, T. Montini, P. Fornasiero, and R. J. Gorte, *Surf. Sci.*, **601**, 2512 (2007).
24. S. Park, R. J. Gorte, and J. M. Vohs, *J. Electrochem. Soc.*, **148**, A443 (2001).
25. Y. Huang, J. M. Vohs, and R. J. Gorte, *J. Electrochem. Soc.*, **151**, A646 (2004).
26. W. Wang, M. D. Gross, J. M. Vohs, and R. J. Gorte, *J. Electrochem. Soc.*, **154**, B439 (2007).

27. M. Boaro, J. M. Vohs, and R. J. Gorte, *J. Am. Ceram. Soc.*, **86**, 395 (2003).
28. J. Canales-Vázquez, S. W. Tao, and J. T. S. Irvine, *Solid State Ionics*, **159**, 159 (2003).
29. S. McIntosh, J. M. Vohs, and R. J. Gorte, *J. Electrochem. Soc.*, **150**, A1305 (2003).
30. S. McIntosh, H. H. He, S.-I. Lee, O. Costa-Nunes, V. V. Krishnan, J. M. Vohs, and R. J. Gorte, *J. Electrochem. Soc.*, **151**, A604 (2004).
31. K. Sasaki and J. Maier, *Solid State Ionics*, **134**, 303 (2000).
32. V. Ruhrup and H.-D. Wiemhofer, *Z. Naturforsch., B: Chem. Sci.*, **61b**, 916 (2006).
33. C. W. Tanner, K.-Z. Fung, and A. V. Virkar, *J. Electrochem. Soc.*, **144**, 21 (1997).